JOURNAL OF CATALYSIS **177,** 147–151 (1998)
ARTICLE NO. CA982086

RESEARCH NOTE

On the Effect of Deactivation on the Kinetics of CO Oxidation by NO over Pt–Rh Catalysts

P. Granger,[1] L. Delannoy, L. Leclercq, and G. Leclercq

Laboratoire de Catalyse Hétérogène et Homogène, URA CNRS 0402, Bât. C3, 59650 Villeneuve d'Ascq Cédex, France

Received January 23, 1998; revised March 10, 1998; accepted March 12, 1998

The CO + NO reaction has been extensively studied over a wide variety of catalysts, in particular on noble metals based catalysts (1, 2). The replacement of platinum and rhodium by less expensive materials exhibiting similar catalytic properties in three-way catalysts (TWC) is of greatest importance from an economical viewpoint, consequently, many investigations focused on this practical interest have been reported in the literature (3, 4). However, both metals are still the most active components in TWCs. Further developments of TWCs seem related both to a better understanding of elementary surface reactions on atomic scale and the existing relationship between surface processes and structure and composition of TWCs. In order to clarify these two fundamental considerations many kinetic and spectroscopic studies were devoted to the CO + NO reaction. Several mechanisms have been proposed to describe the CO + NO reaction in various operating conditions (5–7) because TWCs never operate at steady state. However, there seems to be presently a general agreement on the following mechanism to describe the activity and selectivity of TWCs (8–13) in a wide range of operating conditions. This mechanism includes the preliminary dissociation of NO according to step [3].

$$NO + * \Leftrightarrow NO^* \quad [1]$$

$$CO + * \Leftrightarrow CO^* \quad [2]$$

$$NO^* + * \rightarrow N^* + O^* \quad [3]$$

$$NO^* + N^* \rightarrow N_2 + O^* + * \quad [4]$$

$$NO^* + N^* \rightarrow N_2O + 2^* \quad [5]$$

$$N^* + N^* \rightarrow N_2 + 2^* \quad [6]$$

$$CO^* + O^* \rightarrow CO_2 + 2^*, \quad [7]$$

where $*$ denotes a vacant adsorption site.

[1] To whom correspondence should be addressed. E-mail: catalyse@univ-lille1.fr.

Previous investigations on the kinetics of the CO + NO reaction performed in our laboratory at 300°C under reducing or moderate oxidizing conditions over Pt-only (14), Rh-only, and Pt–Rh catalysts (15) agree with this mechanism. The reactant partial pressure dependencies of the experimental reaction rate has been correctly modelled by Eq. [8] derived from this mechanism. Previous assumptions such as: (i) competitive adsorptions of NO and CO on a single site and, (ii) NO dissociation (step [3]) as rate determining have been considered to establish the rate expression

$$r = \frac{k_3 \lambda_{NO} P_{NO}}{(1 + \lambda_{NO} P_{NO} + \lambda_{CO} P_{CO})^2}, \quad [8]$$

where λ_{CO} and λ_{NO} are respectively the adsorption equilibrium constants of CO and NO and k_3, the NO dissociation rate constant.

In the case of Pt–Rh/Al_2O_3 a more relevant kinetic model has been proposed (15), based on previous infrared observations dealing with the co-adsorption of CO and NO on Pt–Rh/SiO_2. Van Slooten and Nieuwenhuys (16) have suggested that NO is preferentially adsorbed on Rh and CO on Pt. This alternative mechanism can fit more accurately our kinetic data on Pt–Rh/Al_2O_3, freshly prepared, according to the rate equation [9]

$$r = \frac{k_3 \lambda_{NO} P_{NO}}{(1 + \lambda_{NO} P_{NO})(1 + \lambda_{CO} P_{CO})}. \quad [9]$$

Furthermore the adsorption equilibrium constants of NO and CO are respectively similar to those obtained on Rh-only and Pt-only catalysts which is in excellent agreement with the proposals of Van Slooten and Nieuwenhuys (16). It was concluded that Pt and Rh preserve their individual adsorption properties on a fresh catalyst. Hence, the average activity of Pt–Rh/Al_2O_3 has been ascribed to a dilution effect by Pt which considerably lowers the surface Rh activity.

There are presently evidences that the surface composition of bimetallic catalysts is very sensitive to deactivation which occurs on TWCs at high temperature and/or while the

0021-9517/98 $25.00

TABLE 1

Bulk and XPS Composition of Fresh and Sintered Bimetallic Pt–Rh/Al_2O_3 Catalysts

		XPS analysis				
	Bulk composition	Surface composition			B.E. (eV)	
Catalysts	$\left[\frac{Rh}{Rh+Pt}\right]^b$	$\left[\frac{Rh}{Rh+Pt}\right]^b$	$\frac{Pt^a}{Al}$	$\frac{Rh^a}{Al}$	Pt $4d_{3/2}$	Rh $3d_{5/2}$
Fresh	0.27	0.33	2.1×10^{-3}	1.0×10^{-3}	332.1	307.8
Sintered	0.27	0.50	1.0×10^{-3}	1.0×10^{-3}	332.3	307.0

[a] Atomic ratios calculated from the intensities of the photopeaks Al $2p$ from Al_2O_3, Pt $4d_{3/2}$, and Rh $3d_{5/2}$.
[b] Atomic Rh composition.

feedstream composition varies. Several studies mentioned that deactivation leads to both particle growth and surface Rh enrichment (17–19).

A sample of a fresh Pt–Rh/Al_2O_3 catalyst was prepared according to the same procedure used by Kacimi and Duprez (20) who found some indications for the formation of bimetallic Pt–Rh particles and then was deactivated by submitting it to a thermal treatment at 800°C in a mixture of 10 vol% H_2O in N_2 for 16 h. This thermal treatment induced a slight decrease of the specific area from 95.5 to 71 $m^2\ g^{-1}$. As seen in Table 1, XPS measurements performed on these two catalysts do not reveal any significant changes in the binding energies of Pt $4d_{3/2}$ and Rh $3d_{5/2}$ levels. Their comparison with the current values reported in the literature (21) shows that Pt and Rh are mainly in their metallic state on both catalysts. The results of the quantitative analysis by XPS data of the two bimetallic Pt–Rh catalysts using a procedure already reported in Ref. (22) (Table 1) show clearly a Rh enrichment in the layer analyzed by XPS for the sintered sample mainly due to a decrease in the Pt signal. As expected, this thermal treatment resulted in a decrease of the metal dispersion from 0.64 to 0.27, as determined by hydrogen chemisorption. The corresponding average bimetallic particle sizes are 1.4 and 3.4 nm, respectively, on the fresh and sintered catalysts.

The kinetics of the CO + NO reaction has been investigated on the sintered Pt–Rh/Al_2O_3 catalyst in a differential fixed bed flow reactor at 300°C (15) in order to avoid external heat and mass transfer limitations. The space velocity was adjusted to 25000 h^{-1} during the catalyst testing to obtain NO and CO conversions below 14%. It is noticeable that the thermal sintering does not significantly alter the specific activity Pt–Rh/Al_2O_3 (see Table 2) despite the decrease of the metal dispersion by a factor ~2.5. The experimental rates measured at various NO and CO partial pressures are listed in Table 3.

The reaction orders obtained from these data by means of linear regression analysis are −0.33 and −0.12 respectively for CO and NO within the reactant partial pressure ranges used in this study (Table 2). Obviously sintering has a major effect on the formal kinetics of CO oxidation by NO, mainly on the order in NO, but a limited effect on the global reaction rates (Table 2). Sintered Pt–Rh behaves more like Rh/Al_2O_3 which has been shown to exhibit positive order in NO in the range of P_{NO} between 0.5×10^{-3} and 2.0×10^{-3} atm, but negative orders for higher P_{NO} (the maximum rate was obtained for $P_{NO} = 2.5 \times 10^{-3}$ atm). Consequently in the P_{NO} range studied here, the apparent order in NO is negative for the sintered Pt–Rh/Al_2O_3.

The negative order for CO is compatible with both Eqs. [8] and [9], but the negative NO order for the sintered Pt–Rh/Al_2O_3 is inconsistent with Eq. [9].

We have attempted to calculate the rate constant of NO dissociation, k_3, and the adsorption equilibrium constants

TABLE 2

Rates and Reaction Orders for the CO + NO Reaction at 300°C

Catalyst	P_{NO} (10^{-3} atm)	P_{CO} (10^{-3} atm)	Specific[c,e] activity	TOF[d,e]	n[a]	m[a]
0.2 wt% Rh/Al_2O_3[b]	0.5–2.0	3.0–13.6	2.6×10^{-2}	1423	0.80	−0.32
	2.5–3.2	3.0–13.6			<0	−0.32
Fresh 1 wt% Pt-0.2 wt% Rh/Al_2O_3[b]	1.5–5.6	3.0–8.0	2.1×10^{-3}	46	0.40	−0.38
Sintered 1 wt% Pt-0.2 wt% Rh/Al_2O_3	2.0–8.2	4.5–8.8	1.9×10^{-3}	101	−0.12	−0.33

[a] Rate = $k \times P_{NO}^n \times P_{CO}^m$.
[b] From Ref. (15).
[c] CO mol $h^{-1}\ g^{-1}$ catalyst.
[d] CO molec $\cdot\ h^{-1}$ (surface metal at)$^{-1}$.
[e] At T = 300°C with initial $P_{NO} = P_{CO} = 5 \times 10^{-3}$ atm.

TABLE 3

Influence of the Partial Pressures of NO and CO on the Rate of CO Oxidation by NO on Sintered 1 wt% Pt-0.2 wt% Rh/Al_2O_3 ($T = 300°C$, Space Velocity = 25000 h^{-1})

P_{NO}, atm	P_{CO}, atm	r[a], mol g^{-1} h^{-1}
2.0×10^{-3}	4.5×10^{-3}	$(2.4 \pm 0.35) \times 10^{-3}$
4.2×10^{-3}	4.6×10^{-3}	$(1.9 \pm 0.3) \times 10^{-3}$
4.4×10^{-3}	4.7×10^{-3}	$(2.0 \pm 0.3) \times 10^{-3}$
7.4×10^{-3}	4.7×10^{-3}	$(1.95 \pm 0.3) \times 10^{-3}$
8.2×10^{-3}	4.7×10^{-3}	$(2.0 \pm 0.35) \times 10^{-3}$
4.3×10^{-3}	2.6×10^{-3}	$(2.1 \pm 0.35) \times 10^{-3}$
4.3×10^{-3}	4.7×10^{-3}	$(1.9 \pm 0.3) \times 10^{-3}$
4.3×10^{-3}	4.7×10^{-3}	$(1.9 \pm 0.3) \times 10^{-3}$
4.5×10^{-3}	5.8×10^{-3}	$(1.9 \pm 0.3) \times 10^{-3}$
4.5×10^{-3}	7.7×10^{-3}	$(1.6 \pm 0.2) \times 10^{-3}$
4.4×10^{-3}	8.8×10^{-3}	$(1.6 \pm 0.2) \times 10^{-3}$

[a] Rate of CO oxidation by NO, expressed per gram of catalyst, calculated from the CO conversion, T_{CO} according to the equation: $T_{CO} = T_{N_2} + T_{N_2O}/2$, where T_{N_2} and T_{N_2O} are respectively the conversion of NO into N_2 and N_2O.

of NO and CO (λ_{CO} and λ_{NO}) by solving Eqs. [8] and [9], using the graphic and optimisation methods earlier described in Ref. (14). The accuracy on the calculated parameters is about $\pm 20\%$. Only Eq. [8] leads to positive values for k_3, λ_{NO}, and λ_{CO} (Table 4) from the graphic method and converges towards a unique set of values using the optimisation method. In addition, comparable results are obtained from these two methods which allow us to conclude that only competitive adsorptions of CO and NO enable us to model the reactant partial pressure dependencies of the reaction rate. Comparison of λ_{NO} on fresh and sintered bimetallic $Pt–Rh/Al_2O_3$ shows no significant change in λ_{NO} after ageing, it remains close to that obtained on Rh/Al_2O_3, according to the margin of error. On the contrary, on the sintered $Pt–Rh/Al_2O_3$ sample, the value of λ_{CO} is closer to that obtained on Rh/Al_2O_3 than to that on the fresh one, which had been shown to be approximately the same as that obtained on Pt/Al_2O_3 (15).

It may seem surprising that for the fresh $Pt–Rh/Al_2O_3$ the model with noncompetitive adsorptions is favored (see Ref. (15) for arguments) while for the sintered sample only competitive adsorptions are consistent with our experimental results. This apparent contradiction could be removed if sintering strongly modifies the surface of the metal particles and transforms the metal surface where both Pt and Rh coexist together in a metal surface mainly composed of Rh atoms.

A comparative infrared study of CO adsorbed on $Pt–Rh/Al_2O_3$ freshly prepared and after thermal sintering, reveals modifications in the IR band shape of adsorbed CO species. Figure 1 shows the IR spectra recorded on prereduced $Pt–Rh/Al_2O_3$ samples obtained after contact with CO at 25°C for 1 h and outgassing at the same temperature. The assignments of IR bands have been carried out from previous IR studies on Pt-only and Rh-only catalysts (23). For Pt/Al_2O_3, a major band and a less intense one were detected at 2070 and 1850 cm^{-1} which characterised respectively linear and bridged CO species on Pt metal. These corresponding IR bands were located at 2060 and 1890 cm^{-1} on Rh/Al_2O_3; in addition two bands appeared at 2030–2040 and 2100 cm^{-1} due to rhodium gem-dicarbonyl species, $Rh^+(CO)_2$. All these IR observations are in agreement with IR studies already published in the literature (24–27). The spectrum on the fresh $Pt–Rh/Al_2O_3$ sample (Fig. 1.A) is dominated by an IR band at 2070 cm^{-1}. A broad band with a weak maximum at 1840 cm^{-1} is also observed which indicates the formation of respectively linear and bridged CO species mainly on Pt metal. On the sintered sample (Fig. 1.B), the IR band corresponding to the

TABLE 4

Kinetic and Thermodynamic Constants for the Oxidation of CO by NO on Rh and Pt Based Catalysts at 300°C

Catalyst	Rate equation	Slope α	Intercept β	k_3[b]	k_3'[c]	λ_{NO} atm^{-1}	λ_{CO} atm^{-1}
0.2 wt% Rh/Al_2O_3[a]	[8]			225×10^{-3}	12315	472	71
Fresh 1 wt% Pt-0.2 wt% Rh/Al_2O_3[a]	[9]			4.74×10^{-3}	469	505	122
Sintered 1 wt% Pt-0.2 wt% Rh/Al_2O_3	[8]	42.2[d]/174.5[e]	1.14[d]/0.65[e]	13.2×10^{-3}	691	402	97
				11.9×10^{-3}[h]	623[h]	448[h]	85[h]
	[9]	144.7[f]/523.6[g]	1.55[f]/−0.15[g]			−3491	93

[a] From Ref. (15).
[b] Specific rate constant for the dissociation of NO (mol h^{-1} g^1).
[c] Intrinsic rate constant for the dissociation of NO (molec · h^{-1} metal at^{-1}).
[d] From the linear plot $(P_{NO}/r)^{0.5}$ vs P_{CO}.
[e] From the linear plot $(P_{NO}/r)^{0.5}$ vs P_{NO}.
[f] From the linear plot P_{NO}/r vs P_{CO}.
[g] From the linear plot P_{NO}/r vs P_{NO}.
[h] Calculated from the optimisation method.

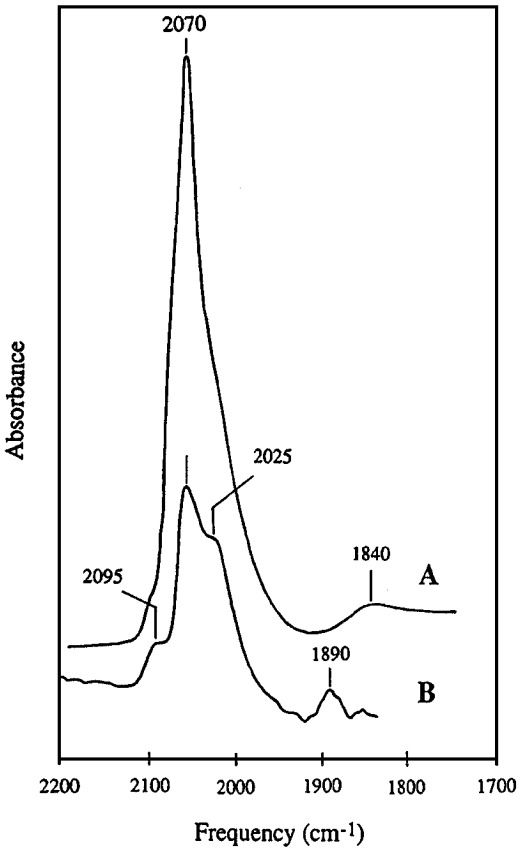

FIG. 1. Infrared spectra of CO adsorbed on a fresh bimetallic $Pt–Rh/Al_2O_3$, A and on a sintered $Pt–Rh/Al_2O_3$ catalyst, B. The samples were reduced "*in situ*" in flowing hydrogen at 500°C, then outgassed under vacuum at 350°C. At the end of this treatment the cell was cooled at room temperature before introducing 1.6×10^{-2} atm CO. The catalysts were maintained in these operating conditions for 1 h before CO evacuation.

linear carbonyl species significantly decreases in intensity and is shifted towards lower frequencies (2060 cm^{-1}) while the CO-bridged band is shifted towards higher frequencies (1890 cm^{-1}). Moreover, the IR bands at 2025 and 2095 cm^{-1} corresponding to the gem-dicarbonyl species clearly appear, but they remain less intense than that corresponding to the linear CO species. All these absorptions are characteristic of CO adsorbed on Rh. On this metal, the relative intensities of the gem-linear bands have been shown to be a function of the metal dispersion (27, 28). The results reported here suggest that Rh is not in very small particles in the sintered sample. As a matter of fact, the spectrum obtained resembles very closely that reported by Barbier *et al.* (29) on Rh/Al_2O_3 with medium metal dispersion (0.48). Finally, all these changes in both location and intensity of IR bands suggest that CO adsorbs mainly on Rh on the sintered $Pt–Rh/Al_2O_3$ catalyst.

Consequently both kinetic and IR results seem to point out a Rh-like behaviour of the sintered $Pt–Rh/Al_2O_3$ catalyst, in contrast to the fresh sample at the surface of which both Pt and Rh coexist. Such a phenomenon could have several explanations. First, a true rhodium surface segregation could be considered if bimetallic particles exist at the surface of $Pt–Rh/Al_2O_3$. For the fresh catalyst, with a metal dispersion of 0.64, the global composition (27.5 at% Rh) clearly indicates that the metal surface must contain a majority of Pt atoms (at least 58%), even if all the Rh atoms were segregated at the surface. On the contrary, for the sintered sample, its lower metal dispersion (0.27) would allow a metal surface mainly composed of Rh atoms if these atoms were segregated at the surface of metal particles. Of course such a total segregation would be a borderline case and, if such an explanation is correct, the segregation is likely to be incomplete. Moreover some separated Pt and Rh particles could be present. Alternatively, if, on the fresh catalyst, bimetallic particles were not formed, different deactivation processes for Pt and Rh could occur. For example the metal Pt particles could sinter to large particles, whereas the Rh particles could sinter less, leading to a global catalyst exhibiting a Rh-like behaviour. Let us note that this latter explanation could still hold even if bimetallic particles are present in the fresh catalyst if sintering in the presence of water leads to dealloying of Pt and Rh atoms.

Going further, a good comparison of the catalytic properties of these two catalysts can only be achieved from the examination of the intrinsic NO dissociation rate constant, k'_3. Let us notice the low value of k'_3 on the sintered $Pt–Rh/Al_2O_3$ which is unexpected since it should be comparable to that of Rh/Al_2O_3, whereas, in fact, k'_3 is approximately 20 times lower on sintered $Pt–Rh/Al_2O_3$ than on Rh/Al_2O_3. Such a variation in k'_3 could arise from the structure sensitivity of the dissociation of adsorbed NO that was already mentioned by Peden *et al.* on Rh (111) and (110) single crystals (30).

To conclude, both the physicochemical characterization and the kinetic study of the CO + NO reaction evidenced a major surface composition modification of a $Pt–Rh/Al_2O_3$ catalyst after thermal sintering in the presence of water. Such a treatment seems to lead to a Rh enrichment of the surface of the metal particles. This shows that kinetic studies can provide relevant information by deriving a rate expression and calculating parameters which can further be used, not only in the field of kinetic modelling, but also as a tool for the characterization of the surface composition of bimetallic catalysts.

ACKNOWLEDGMENTS

We thank Drs. G. Mabilon and M. Prigent for their contribution to this work and also Dr. H. Praliaud for the interpretation of the infrared measurements.

REFERENCES

1. Shelef, M., and Graham, G. W., *Catal. Rev. Sci. Eng.* **36**, 433 (1994).
2. Taylor, K. C., *Catal. Rev. Sci. Eng.* **35**, 144 (1993).

3. Adams, K. M., and Gandhi, H. S., *Ind. Eng. Chem. Prod. Res. Dev.* **22**, 207 (1983).
4. Gandhi, H. S., Yao, H. C., and Stepien, H. K., *in* "ACS Sympos. Ser.," Vol. 178 (A. T. Bell and L. Hegedus, Eds.), p. 143. Am. Chem. Soc., Washington, DC, 1982.
5. Klein, R. L., Shwartz, S. B., and Schmidt, L. D., *J. Phys. Chem.* **89**, 4908 (1985).
6. Aldoch, W., and Linz, H. G., *Surf. Sci.* **78**, 69 (1978).
7. Dubois, L. H., Hansma, P. K., and Somorjai, G. A., *J. Catal.* **65**, 318 (1980).
8. Masel, R. I., *Catal. Rev. Sci. Eng.* **28**, 335 (1986).
9. Hecker, W. C., and Bell, A. T., *J. Catal.* **85**, 389 (1984).
10. Hecker, W. C., and Bell, A. T., *J. Catal.* **59**, 223 (1979).
11. Cho, B. K., Shank, B. H., and Bailey, J. E., *J. Catal.* **115**, 486 (1989).
12. Oh, S. E., Fisher, G. B., Carpenter, J. E., and Goodman, D. W., *J. Catal.* **100**, 360 (1986).
13. Ng, K. Y. S., Belton, D. N., Schmieg, S. J., and Fisher, G. B., *J. Catal.* **146**, 394 (1994).
14. Granger, P., Dathy, C., Lecomte, J. J., Prigent, M., Mabilon, G., Leclercq, L., and Leclercq, G., *J. Catal.* **173**, 304 (1998).
15. Granger, P., Dathy, C., Lecomte, J. J., Leclercq, L., and Leclercq, G., *J. Catal.*, in press.
16. Van Slooten, R. F., and Nieuwenhuys, B. E., *J. Catal.* **122**, 429 (1990).
17a. Kim, S., and D'Aniello, M. J., Jr., *Appl. Catal.* **56**, 23 (1989).
17b. Kim, S., and D'Aniello, M. J., Jr., *Appl. Catal.* **56**, 45 (1989).
18. Powell, B. R., and Chen, Y. L., *Appl. Catal.* **53**, 233 (1989).
19. Malm, J. O., and Bovin, J. O., *Microanal. Microstruct.* **1**, 387 (1990).
20. Kacimi, S., and Duprez, D., *in* "Catalysis and Automotive Pollution Control II" (A. Crucq, Ed.), Vol. 71, p. 581. Elsevier, Amsterdam, 1991.
21. Wagner, C. D., Riggs, W. M., Davis, L. E., and Moulder, J. F., "Hand Book of X-Ray Photoelectron Spectroscopy" (G. E. Muilenberg, Ed.), Perkin Elmer, Palo Alto, CA, 1979.
22. Grimblot, J., *in* "Analyse des surfaces des solides," p. 125. Masson, Paris, 1995.
23. Unpublished results obtained at the Institut de Recherche sur la Catalyse.
24. Anderson, J. A., and Rochester, C. H., *Catal. Today* **10**, 275 (1991).
25. Alikina, G. M., Davidov, A. A., Sazonova, I. S., and Popovskii, V. V., *React. Kinet. Catal. Lett.* **27**, 279 (1985).
26. Yang, A. C., and Garland, C. W., *J. Phys. Chem.* **61**, 1504 (1957).
27. Yates, D. J. C., Murel, L. L., and Prestridge, E. B., *J. Catal.* **84**, 41 (1979).
28. Solymosi, P., *J. Phys. Chem.* **89**, 4789 (1985).
29. Barbier, J., Dumas, J. M., Géron, C., and Hadrane, H., *Appl. Catal.* **67**, L1 (1990).
30. Peden, C. H. F., Belton, D. N., and Schmieg, S. J., *J. Catal.* **155**, 204 (1995).